



2nd Mediterranean Conference on Fracture and Structural Integrity

# Combination of discrete and finite element method to simulate damage in galvanised steel

Leandro Friedrich<sup>a</sup>, Angélica Colpo<sup>b</sup>, Sabrina Vantadori<sup>c</sup>, Andrea Zanichelli<sup>c</sup>,  
Vittorio Di Cocco<sup>d\*</sup>, Francesco Iacoviello<sup>d</sup>, Ignacio Iturrioz<sup>b</sup>

<sup>a</sup>Department of Mechanical Engineering, Federal University of Pampa, Av. Tiaraju 810, 97546-550 Alegrete, Brazil

<sup>b</sup>Program of Mechanical Pos-Graduation, Federal University of Rio Grande do Sul, Sarmiento Leite 425, 90040-060 Porto Alegre, Brazil

<sup>c</sup>Department of Engineering & Architecture, University of Parma, Parco Area delle Scienze 181/A, 43124 Parma, Italy

<sup>d</sup>DICeM, Università di Cassino e del Lazio Meridionale, Via G. Di Biasio, 43, 03043 Cassino (FR), Italy

## Abstract

In the present paper, the bending behaviour of a hot-rolled hyper-sandelin steel, subjected to hot-dip galvanizing (HDG), is numerically simulated in Ansys LS-DYNA environment by combining the Discrete Element Method (DEM) with Finite Element Method (FEM). The coating examined is composed by different layers: the layers with a ductile behaviour are modelled by using elastoplastic constitutive laws for the FEs, whereas the layers with a quasi-brittle behaviour are simulated by using DEs. Such an approach shows quite satisfactory results and it can be promising as a numerical tool to be used by HDG industry, being accurate to estimate the damage of galvanized steel.

© 2022 The Authors. Published by Elsevier B.V.

This is an open access article under the CC BY-NC-ND license (<https://creativecommons.org/licenses/by-nc-nd/4.0>)

Peer-review under responsibility of the MedFract2Guest Editors.

*Keywords:* Finite Element Method; Discrete Element Method; zinc-based coatings; plasticity; non-linear fracture mechanics.

## 1. Introduction

Steel remains one of the most used materials for construction of automobiles, industrial machinery and for civil construction in general due to its high strength and durability. However, the action of different environments on steel

\* Corresponding author.

E-mail address: [v.dicocco@unicas.it](mailto:v.dicocco@unicas.it)

can lead to a corrosion process. One of the main methods to prevent corrosion are the zinc coatings, offering increased corrosion resistance at moderate costs (Shibli et al. (2015)). The so-called galvanized steels are produced by a hot-dip galvanizing process, where steel parts are hot dipped in a bath of molten zinc for a given time interval at a predefined temperature. Therefore, zinc coating protects steel by a cathodic reaction corroding itself instead of steel, due to the different electromechanical potential of these two materials (active protection) (Vantadori et al. (2022)).

When the steel is dipped in the zinc bath (industrial standard temperature of 450 °C), a series of zinc-iron alloy layers are formed (Fig.1), consisting in the following intermetallic phases: gamma ( $\Gamma$  - 75%Zn–25% Fe), delta ( $\delta$  - 90% Zn–10% Fe), zeta ( $\zeta$  - 94%Zn–6% Fe), and eta ( $\eta$  - 100%Zn) (Shibli et al. (2015)). Such intermetallic phases are distinguished by microstructure, mechanical and thermal properties (Reumont et al. (2001)).

In the present paper, the stable crack propagation in the coating layers of a galvanized hyper-sandelin steel is numerically investigated by using a numerical model that combines the Finite Element Method (FEM) with the Lattice Discrete Element Method (LDEM). More precisely, the  $\delta$  and  $\zeta$  layers are simulated by using discrete elements, which allows to capture the nucleation and stable propagation of cracks, whereas the rest of the body is modelled with finite elements. The simulation is performed on the experimental campaign conducted by Di Cocco et al. (2014), where a galvanized plate is subjected to a constant bending moment. A comparison between the cracks paths experimentally observed by a Light Optical Microscopy (LOM) and that numerically obtained is performed.

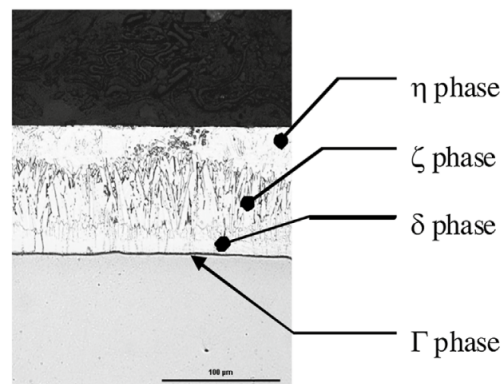


Fig. 1. Intermetallic phases present in a typical hot-dip galvanized coating (Carpinteri et al. (2016)).

## 2. Lattice Discrete Element Method (LDEM)

The basic formulation of the Lattice Discrete Element Method (LDEM) used in the present work has been presented in many research papers as, for example, in the works by Iturrioz et al. (2013) and Koteski et al. (2020). Thus, only a brief description of the method is presented below.

The LDEM consists in the discretization of the continuum as a 3D-array of nodes linked by uniaxial elements (also named bars in the following) spatially arranged, and with masses concentrated at the nodes. These bars are organized in a cubic arrangement (Fig. 2a) that is cubic cells with nine nodes, as proposed by Nayfeh and Hefzy (1978). Each node has three degrees of freedom, corresponding to the nodal displacements in three orthogonal directions.

Each unidirectional element has a constitutive law that relates internal force to the displacement, as is shown in Fig. 2b, where  $F$  is the bar axial force and  $\varepsilon$  is the axial strain. This constitutive law is based on the proposal made by Hillerborg et al. (1976). The area under such a curve (triangle OAB in Fig. 2b) is related to the energy density needed to fracture the area of influence of the bar. Once the energy density equals the fracture energy, the element fails and loses its load carrying capacity. Under compression, the material behaves linearly. Thus, this nonlinear constitutive model allows both to reproduce the material damage and the element failure when a critical force condition is reached.

The bilinear law shown in Fig. 2b directly depends on three local parameters, that is:  $EA_i$ ,  $\varepsilon_{ii}$  and  $\varepsilon_p$ . The bar specific stiffness,  $EA_i$ , is function of both the Young's modulus,  $E$ , and the cross-section area of the bar,  $A_i$ , where  $i$  is equal to  $n$  for normal bar and to  $d$  for diagonal bar. The ultimate strain,  $\varepsilon_u$ , is the strain value for which the element loses its

load bearing capacity (that is the bar breaks), whereas the critical strain,  $\varepsilon_p$ , is the strain at the crack initiation, function of a characteristic length of the material,  $d_{eq}$ .

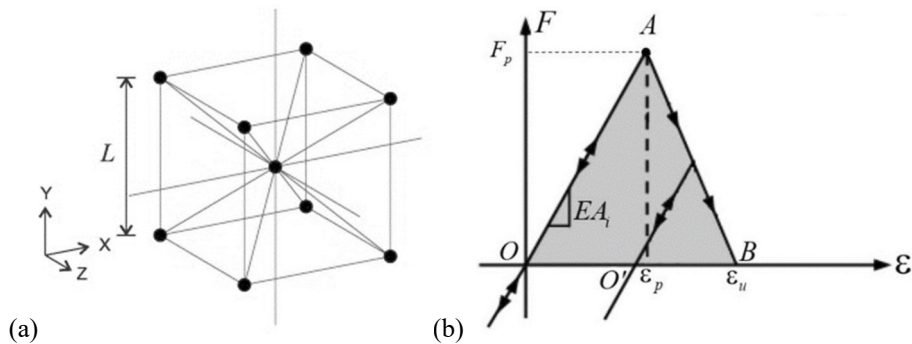


Fig. 2. LEDM: (a) Basic cubic module employed in the discretisation and (b) bilinear constitutive law attributed to the bars.

### 2.1. LDEM in the Ansys-DYNA environment

The LDEM is implemented into the Ansys-LS DYNA environment (ANSYS (2011)) (named LDEM-DYNA in the following) in order to develop a hybrid model, that is LDE model combined with FE model. More precisely, the region where the fracture is expected to occur is modelled by means of discrete elements, whereas the rest of the model is discretised by using finite elements (Zanichelli et al. (2021)).

The bars, which represent the basic LDEM module (see Fig. 2a), are modelled in Ansys LS-DYNA by using discrete spring elements (COMBI165). The COMBI165 is able to generate a force that depends on the bar displacement. In LDEM-DYNA the mass of the simulated body is concentrated in the COMBI165 nodes, by using the MASS166 element. The mass value depends on the node position within the basic module (Zanichelli et al. (2021)).

For numerical simulation, a statistical variation should be included in the properties of the material in order to take into account possible imperfections present into the material. In the LDEM-DYNA, such an aspect is taken into account by considering the fracture energy randomly distributed in 3D with a Weibull probability. Details may be found in Puglia et al. (2019).

### 3. Experimental campaign examined

The experimental campaign examined was performed by Di Cocco et al. (2014) on galvanized specimens under constant bending moment, applied by using a non-standardized device (Duncan et al. (1999)). The bending moment against half bending angle was experimentally measured, reaching a maximum half bending angle equal to 34°. Hot-rolled steel plate specimens (80 x 25 x 3 mm) were used, being the specimens dipped in a pure-zinc bath for different dipping times (equal to 15, 60, 180, 360, and 900 s).

Using LOM, the phase thicknesses of each intermetallic phase were measured. For the dipping time equal to 15s, the following phase thicknesses were measured:  $\delta = 13 \mu\text{m}$ ,  $\zeta = 4 \mu\text{m}$  and  $\eta = 19 \mu\text{m}$ .

### 4. LDEM-DYNA model

The bending testing performed on galvanised plates is here numerically simulated in the Ansys LS-DYNA environment. More precisely, the specimen characterised by a dipping time equal to 15s is numerically simulated. A bi-dimensional model is employed, due to the fact that the problem is characterized by a plain strain condition.

Fig. 3a shows the geometry of the model and element types used to represent each material, where  $t'$  represents the sum of the thickness of the intermetallic phases equal to 26  $\mu\text{m}$ . The steel, the  $\eta$  phase and all the intermetallic

phases in compression are simulated by using finite elements (SOLID164), whereas the  $\delta$  and the  $\zeta$  phases, which are characterised by quasi-brittle behaviour, are modelled by using discrete elements.

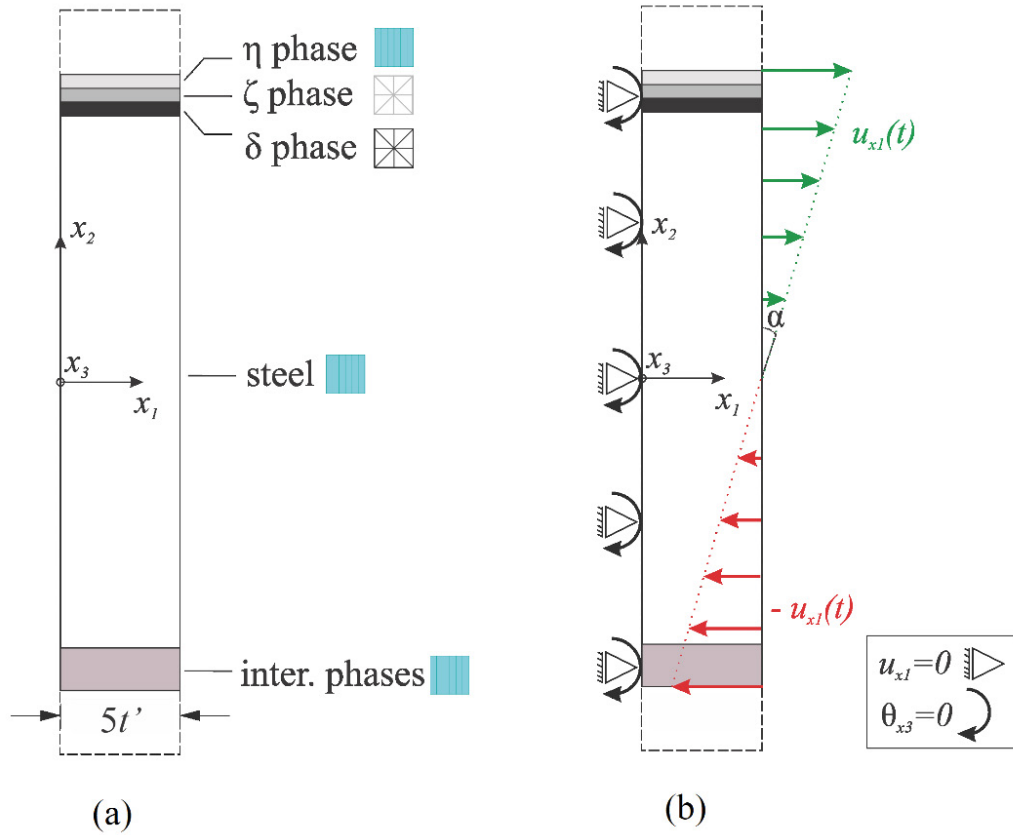


Fig. 3. LDEM-DYNA model: (a) geometry and element types; (b) boundary conditions.

Fig. 3b shows the boundary conditions applied in order to have a constant bending moment in the model, that is the same loading condition characterising the specimen during the experimental campaign. Along the  $x_2$  axis, the nodal displacement in  $x_1$  direction and the nodal rotation around  $x_3$  direction are equal to zero, whereas along the axis parallel to  $x_2$ , at a distance  $5l'$  from  $x_2$ , a linear prescribed displacement,  $u_{x1}(t)$ , is applied.

In Table 1 are listed the number of elements employed and the behaviour (constitutive law) assumed for each intermetallic phase and for the support (steel). In the LDE model the cubic module length,  $L$ , is assumed to be equal to  $1 \mu\text{m}$ . More details about the above laws can be found in Vantadori et al. (2022).

Table 1. Discretization parameters.

	FEs No.	DEs No.	Constitutive law type
Steel	3900	-	Elastic-plastic with strain hardening (Vantadori et al. (2022))
Inter. phase	520	-	Perfectly plastic (Vantadori et al. (2022))
$\delta$ phase	-	1690	Bilinear law (Table 2)
$\zeta$ phase	-	520	Bilinear law (Table 2)
$\eta$ phase	520	-	Perfectly plastic (Vantadori et al. (2022))

As far as the parts simulated by LDEM are concerned, the parameters characterising their constitutive laws are listed in Table 2. More precisely, the parameter  $E$  and  $K_{IC}$  can be found in Vantadori et al. (2022) and Ploypech et al. (2012), respectively.

Table 2. LDE model parameters.

	$E$ [GPa]	$K_{IC}$ [MPam <sup>0.5</sup> ]	$d_{eq}$ [m]	$\varepsilon_p$ [-]	$\varepsilon_r$ [-]
$\delta$ phase	140	2.0	$1.980(10)^{-5}$	$3.32(10)^{-3}$	$4.26(10)^{-2}$
$\zeta$ phase	107.5	4.0	$36.33(10)^{-5}$	$2.03(10)^{-3}$	$47.70(10)^{-2}$

## 5. Results and discussion

In Fig. 4, the damage distribution and failure configuration of the tensile side of the specimen examined is reported. The broken bars are coloured in red, the damaged bars in orange and the undamaged bars in cyan. In correspondence of a half bending angle equal to  $34^\circ$ , a maximum displacement ( $u_{xI} = u_{max}$ ) equal to  $0.5(10)^{-6}$  m is applied. Different values of the displacement level are considered, and more precisely: 25, 50, 75 and 100% of  $u_{max}$ . From Fig. 4 it can be observed that:

- when  $u_{xI}$  is equal to 25% of  $u_{max}$  (Fig. 4(a)), the damage is distributed and mainly concentrated along the  $\zeta$  phase;
- when  $u_{xI}$  is equal to 50% of  $u_{max}$  (Fig. 4(b)), it is possible to observe the nucleation of two micro-cracks, in the  $\delta$  and  $\zeta$  phases. In addition, more damaged bars appears on the left side of the specimen;
- when  $u_{xI}$  is equal to 75% of  $u_{max}$  (Fig. 4(c)), a macro-crack propagates in a stable way. At the same time, another micro-crack is visible in the  $\delta$  phase (right-hand side of the specimen);
- when  $u_{xI}$  is equal to 100% of  $u_{max}$ , that is in the failure configuration (Fig. 4(d)), a second macro-crack is visible in the specimen.

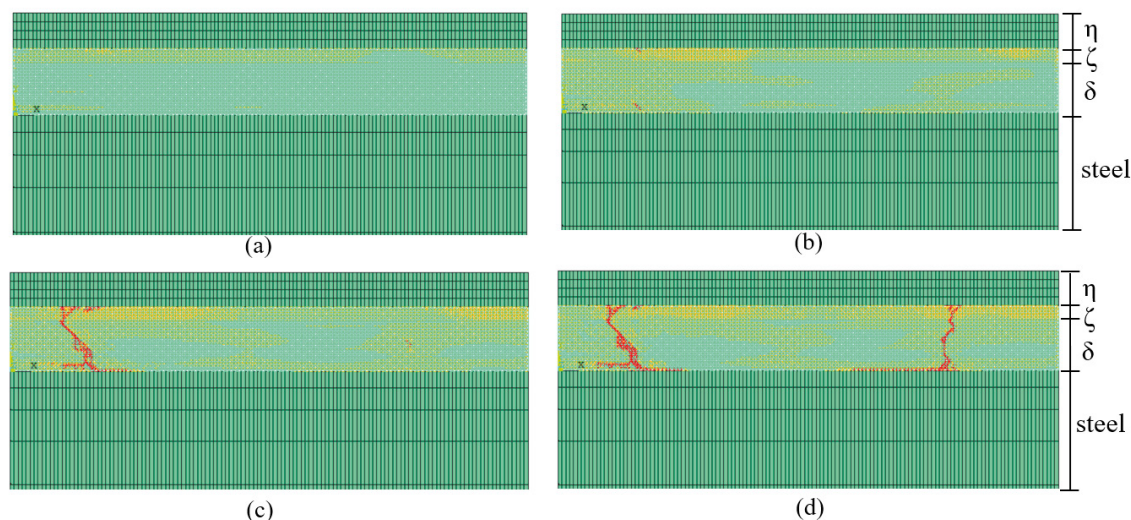


Fig. 4. Cracked configuration at: (a) 25% , (b) 50%, (c) 75% and (d) 100% of the maximum displacement,  $u_{max}$ .

Fig. 5a shows the failure configuration obtained by LDEM-DYNA, whereas Fig. 5b shows the metallography obtained at the end of the test by means of the LOM (only the tensile side is reported).

It can be observed that Mode I cracks are present both in the experimental sample and in the numerical model. By measuring the distance between two cracks,  $d$ , in the numerical model it is twice the experimental one, although a region characterised by an incipient crack (orange region) can be observed in Fig 5b. By measuring the distance

between the centre of such a region and the above cracks, a value of  $d' = 40 \mu\text{m}$  is obtained, that is very close to the experimental one. The results obtained show the effectiveness of the proposed model to capture the damage evolution process in the galvanized specimen.

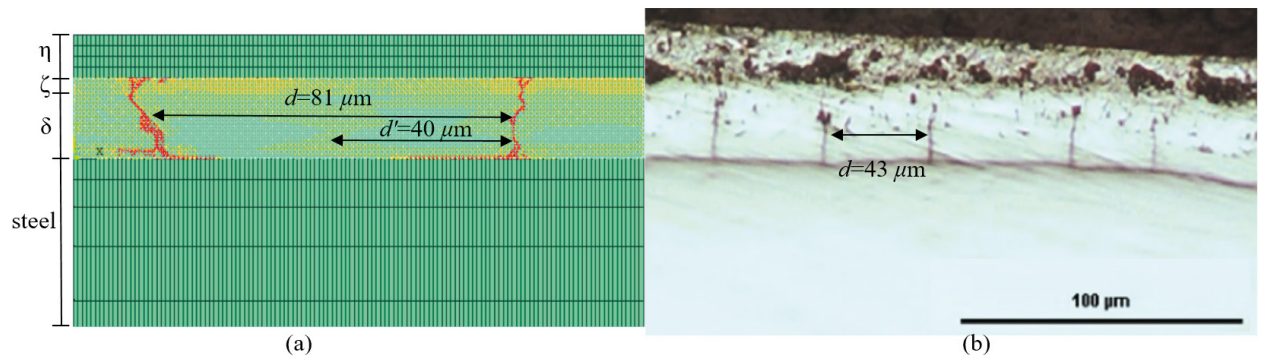


Fig. 5. Comparison between (a) numerical and (b) experimental failure configurations.

## 6. Conclusions

In this work, a hybrid FE-LDE model has been proposed to simulate the damage process of a pure zinc-based galvanized steel specimen. The numerical model developed has shown to be able to capture the damage process in a zinc-based coating with a high accuracy. As a matter of fact, the model has been able to estimate both the Mode of stable crack propagation and the distance between two adjacent cracks.

## References

- ANSYS LS-DYNA User's Guide (v14.0), 2011.
- Carpinteri, A., Di Cocco, V., Fortese, G., Iacoviello, F., Natali, S., Ronchei, C., Scorza, D., Vantadori, S., 2016. Kinetics of Intermetallic Phases and Mechanical Behavior of ZnSn3% Hot-Dip Galvanization Coatings. *Advanced Engineering Materials*, 18, 2088-2094.
- Di Cocco, V., Iacoviello, F., Natali, S., 2014. Damaging micromechanisms in hot-dip galvanizing Zn based coatings. *Theoretical and Applied Fracture Mechanics*, 70, 91-98.
- Duncan J.L., Ding S.-C., Jiang W.L., 1999. Moment-curvature measurement in thin sheet-part I: equipment. *International Journal of Mechanical Sciences*, 41, 249-260.
- Hillerborg, A., Modeer, M., Petersson, P.E., 1976. Analysis of crack formation and crack growth in concrete by means of fracture mechanics and finite elements. *Cement and Concrete Research*, 6 (6), 773-781.
- Iturrioz, I., Lacidogna, G., Carpinteri, A. 2013. Experimental analysis and truss-like discrete element model simulation of concrete specimens under uniaxial compression. *Engineering Fracture Mechanics*, 110, 81-98.
- Kosteski, L.E., Iturrioz, I., Lacidogna, G., Carpinteri, A. 2020. Size effect in heterogeneous materials analyzed through a lattice discrete element method approach. *Engineering Fracture Mechanics*, 232, 107041.
- Nayfeh, A.H., Hefzy, M.S., 1978. Continuum modeling of three-dimensional truss-like space structures. *AIAA Journal*, 16 (8), 779-787.
- Ploypetch, S., Boonyongmaneerat, Y., Jearanaisilawong, P., 2012. Crack initiation and propagation of galvanized coatings hot-dipped at 450 °C under bending loads. *Surface & Coatings Technology*, 18, 3758-3763.
- Puglia, V. B., Kosteski, L. E., Riera, J. D., Iturrioz, I., 2019. Random field generation of the material properties in the lattice discrete element method. *Journal of Strain Analysis for Engineering Design*, 54 (4), 236–46.
- Reumont, G., Voct, J.B., Iost, A., Foct, J., 2001. The effects of an Fe-Zn intermetallic-containing coating on the stress corrosion cracking behaviour of a hot-dip galvanized steel. *Surface and coatings technology*, 139, 265-271.
- Shibli, S.M.A., Meena, B.N., Remya, R., 2015. A review on recent approaches in the field of hot dip zinc galvanizing process. *Surface & Coatings Technology*, 262, 210-215.
- Vantadori, S., Zanichelli, A., Ronchei, C., Scorza, D., Di Cocco, V., Iacoviello, F., 2022. Numerical Simulation of Traditional and Technological Zinc-Based Coatings: Part I. *Advanced Engineering Materials*, 2101619.
- Zanichelli A., Colpo A., Friedrich L., Iturrioz I., Carpinteri A., Vantadori S., 2021. A Novel Implementation of the LDEM in the Ansys LS-DYNA Finite Element Code. *Materials*, 14, 7792.